Applications of Automated Mineralogy in Beneficiation of the Sayona's Lithium Deposit in the Abitibi Region of Québec, Canada

Antonio Di Feo, Maziar Sauber, Shahrokh Shahsavari, Jarrett Quinn, and Tassos Grammatikopoulos

Abstract

Ore deposits are complex and display a high degree of variability which impact their beneficiation. Automated mineralogy (AMIN), which includes ore characterization, mineral and textural quantification, grain size, and mineral liberation in relation to the grinding and beneficiation, is an integral part of the mineral processing industry for the understanding of critical minerals, and base metal sulfides, etc. The data obtained from AMIN can be linked to metallurgical response and used to guide and explain test results, which can help in flowsheet development, process design, and optimization.

This study provides a case study on a lithium ore sample from Quebec, Canada. Mineralogically limited (predicted) grades and recoveries were used as a proxy for beneficiation (e.g., flotation) characterization. Through laboratory testwork, the sample, categorized by size fractions, the correlation between mineralogy and mineral recovery concerning modal mineralogy, grain size, and liberation properties were demonstrated.

For this sample, spodumene was >80% liberated at −300/+150 μm (micrometers) and −150/+75 μm grain size fractions. The flotation recoveries of lithium at 80% passing 205 μm (100% passing 300 μm) and 80% passing 135 μm (100% passing 180 μm) were not significantly different (confirmed with *t*-test). The mineralogical data indicate that there is potential to improve the recovery and grades of lithium with flotation.

Keywords

Automated Mineralogy · Mineral Processing · Critical metals

1 Introduction

Since the start of the twentieth century, the average temperature of the earth has increased by 1 degree Celsius and continues to increase. Increase in the average temperature is causing global weather changes such as precipitation, snow and ice extent, heavy rains, heat waves, and severe thunderstorms. Global warming can contribute to the intensity of heat waves by the higher number of extremely hot days. This results in the increase in the evaporation leading to severe droughts. More droughts create dry fields which become prone to fire [1]. The higher temperatures are caused by greenhouse gases (GHG) resulting from the use of fossil fuels. The world's energy demand is set to at least double over the next 20 years, while fossil fuels are finite. Therefore, research in cleaner technologies has been ongoing to mitigate the effects of global warming and move toward a fossil fuel-free economy.

A. Di Feo (✉) · M. Sauber · S. Shahsavari
Natural Resources Canada, CanmetMINING, Ottawa, ON, Canada
e-mail: tony.difeo@nrcan-rncan.gc.ca

J. Quinn
Sayona Inc., La Motte, QC, Canada

T. Grammatikopoulos
SGS Canada Inc., Lakefield, ON, Canada

Proceedings of the 62nd Conference of Metallurgists, COM 2023, https://doi.org/10.1007/978-3-031-38141-6_72

Most of the clean technologies such as batteries, electric vehicles, and power storage systems use lithium in their structures. Therefore, advances toward the use of clean technologies result in a higher demand for lithium minerals [2]. The utilization of lithium-ion batteries (LiBs) is needed for industrial growth to reduce negative impacts on the climate. In addition to LiBs, lithium is also used in pharmaceuticals in the treatment of the bipolar disorder, synthesis of vitamin A, and organic compounds. Furthermore, due to its high specific energy and low density, lithium is widely used in aerospace industries. It serves as a heat transfer medium in cooling systems and is utilized in the fabrication of aviation parts, as a fluxing agent in ceramics and glass manufacturing, manufacture of lubricants, and as a coolant in reactors in the nuclear industries [3–7].

Lithium economic deposits are categorized as lithium brines (salars, oilfield, and geothermal), sediment-hosted deposits (hectorite and jadarite), as well as pegmatites and highly differentiated granites. Hard rock lithium deposits are extracted through underground and open-pit mining [8]. Lithium is found in minerals such as spodumene, amblygonite, zinnwaldite, petalite, and lepidolite [9].

In order to meet the increasing demand for lithium, there is a requirement to optimize the beneficiation of lithium ores [2, 3]. Froth flotation is an important process for the recovery of lithium minerals from their ores [10]. Flotation was used for Portuguese ores (Barroso) resulting in high-lithium-grade concentrates [11]. The metallurgy of spodumene for a Spanish ore (Vilatuxe pegmatite) was optimized using flotation. The concentrates produced had a grade of about 6.5% Li_2O [12]. Anionic collectors, for example, oleic acid, sodium oleate, sulfonated, and phosphorated fatty acids are used for the flotation of spodumene from pegmatite ores [2]. Spodumene recoveries greater than 90% and concentrate grades of 6.52% Li_2O can be obtained with oleic acid [2].

The mineralogy of hard rock lithium deposits is not always well understood given the internal variability of the deposits. Exploration and mining companies rely heavily on geochemistry to delineate the reserves. If detectable amounts (>1–2%) are present, conventional techniques such as X-ray diffraction (XRD) can provide guidance to the main lithium phases (e.g., spodumene, petalite). However, other lithium-bearing minerals such as phosphates, micas, and tourmaline can contain significant lithium concentrations and may not be identified with the XRD properly if they occur in low-grade. For example, XRD can identify lepidolite group micas, but also muscovite mica which can host considerable lithium, and therefore, the results can be misleading. Micas form solid solution series and do not have a fixed lithium concentration. Moreover, even if the bulk mineralogy is known, geochemical analyses cannot be properly used to determine the lithium minerals due to the presence of a number of lithium minerals in the deposits. Automated mineralogy can be used to improve the understating of the mineralogical characteristics, identify low-grade lithium-bearing minerals, and determine the liberation of the main and subordinate lithium phases, and gangue minerals. However, SEM-based instruments cannot detect lithium. Therefore, it is critical that AMIN is coupled with XRD and mineral chemistry [13]. SGS has added a Tescan Integrated Mineral Analyzer (TIMA-X) which uses strict definitions and Al/Si ratios [13, 14] to simulate and define the presence and quantities of spodumene, petalite, and cookeite, differentiate muscovite from lepidolite, detect beryl, and other minor minerals which may be critical in the downstream processes. These are carried out with a higher degree of confidence compared to other tools like QEMSCAN.

Electron probe micro-analyses (EPMA) are used to determine the major elements of the various minerals, e.g., FeO in spodumene. For example, low FeO concentrations may be suitable for the ceramics and glass industry. Laser Ablation by Inductively Coupled Plasma Mass Spectrometry (LA-ICP-MS) is used to determine not only the concentration of lithium but other low-grade elements such as Ga, Cs, and Rb in spodumene, petalite, micas, phosphates, and other minerals. The data are then coupled to calculate the lithium distribution and evaluate the mineralogy of the deposit. Spodumene is the most common and abundant lithium mineral with the highest concentration of lithium. Lithium production can be influenced by the accurate mineralogical characterization of spodumene deposits.

[13]. Automated mineralogy has been used to quantify mineralogical attributes of various projects including lithium minerals [13–15].

In this article, the mineralogy and beneficiation of a hard rock spodumene-bearing pegmatite ore (HG-B zone) from Sayona Québec's North American Lithium Project are discussed. The North American Lithium Project is located in the Abitibi region of Québec, Canada. Sayona Québec is a wholly owned subsidiary of Sayona Mining Limited, which is a publicly traded company on the Australian Stock Exchange.

Table 1 Mineral abundance by size fraction and calculated head for HG-B ore

Mineral/Fraction	Combined	+300 μm		−300/+150 μm		−150/+75 μ		−75 μm	
Mass Size Distribution (%)	100	181		33.5		20.8		27.7	
Sample/Fraction	Combined	Fraction	Sample	Fraction	Sample	Fraction	Sample	Fraction	Sample
Spodumene	13.4	18.6	3.4	15.6	5.2	12.1	2.5	8.42	2.33
Petalite	0.00	0.00	0.00	0.00	0.00	0.00	0.00	0.01	0.00
Quartz	26.8	30.2	5.5	29.7	10.0	27.2	5.6	20.7	5.7
K-felds pars	15.3	12.2	2.2	14.5	4.9	16.4	3.4	17.6	4.9
Albite	38.1	35.1	6.3	35.5	11.9	38.8	8.1	42.6	11.8
Muscovite	2.01	1.83	0.33	1.65	0.55	1.74	0.36	2.77	0.77
Lepidolite	1.50	0.86	0.16	1.24	0.42	1.31	0.27	2.37	0.66
Biotite	0.72	0.19	0.04	0.19	0.07	0.26	0.05	2.06	0.57
Chlorite	0.39	0.13	0.02	0.17	0.06	0.32	0.07	0.87	0.24
Amphiboles	0.25	0.14	0.03	0.24	0.08	0.26	0.06	0.31	0.09
Garnet	0.65	0.37	0.07	0.66	0.22	0.76	0.16	0.75	0.21
Tourmaline	0.01	0.00	0.00	0.01	0.00	0.01	0.00	0.03	0.01
Calcite	0.43	0.21	0.04	0.22	0.07	0.43	0.09	0.81	0.23
Apatite	0.02	0.00	0.00	0.04	0.01	0.01	0.00	0.03	0.01
Columbite	0.04	0.00	0.00	0.08	0.03	0.01	0.00	0.06	0.02
Sulphides	0.06	0.12	0.02	0.01	0.00	0.06	0.01	0.09	0.03
Other	0.32	0.11	0.02	0.24	0.08	0.31	0.06	0.55	0.15
Total	100	100	18.1	100	33.5	100	20.8	100	27.7

2 Mineralogy of the Feed

The mineralogical analysis was conducted with a TIMA-X, Electron Probe Micro-Analysis (EPMA), and LA by ICP-MS. Chemical assays for major elements were determined by XRF while the sodium peroxide ICP-AES was used to measure Li. The sample was stage crushed to a P_{80} of approximately 300 μm. Four size fractions, including +300 μm, −300/+150 μm, −150/+75 μm, and −75 μm, were prepared based on the mass distribution of the sample for mineralogical examination. Note that TIMA does not detect lithium. The Al/Si ratios were used to simulate and identify the presence of spodumene and the lack of petalite [13, 14]. X-ray diffraction analysis was conducted on the sample to validate the presence of spodumene. Note that there is no other Al-Si mineral that might interfere with the identification of spodumene. The presence of spodumene was also verified with the EPMA and LA-ICP-MS analyses presented below.

2.1 Mineralogical Parameters from the TIMA

Mineral abundance is presented in wt% by size fraction and calculated head (Table 1). The HG-B (calculated head) consists of spodumene (13.4%), quartz (26.8%), K-feldspars (15.3%), albite (38.1%), muscovite (2%), lepidolite (1.5%), and trace amounts (<1%) of other minerals.

The P_{80} (Table 2) for petalite is 267 μm, spodumene 276 μm, muscovite/lepidolite 144 μm, quartz 265 μm, K-feldspars 223 μm, and albite 242 μm.

For the purposes of this analysis, particle liberation is defined based on 2D particle area percent. Particles are classified into the following groups (in descending order) based on mineral-of-interest area percent: pure (100% of the total particle area is, e.g., spodumene), free (≥95% is spodumene) and liberated (≥80% is spodumene). The non-liberated grains have been classified according to association characteristics, where binary association groups refer to particle area percent greater than or equal to 95% of the two minerals or mineral groups. The complex groups refer to particles with ternary, quaternary, and greater mineral associations including the mineral of interest.

Figure 1 illustrates the liberation and association of spodumene by size fraction and calculated head. Liberated (pure, free, and liberated) spodumene calculated for the head sample accounts for 11.1% (out of the 13.4% of the total mass or ca. 83% by normalized mass) in the sample. Liberated spodumene accounts for 2.6%, 4.3%, 2.1%, and 2.1% for the coarse (+300 μm) to fine (−75 μm) size fraction, respectively. The remainder of the spodumene mass occurs as middling particles with albite

Table 2 Median and P_{80} grain size (μm) of selected minerals calculated for the head HG-B ore

Grain Size (μm)	Median	P_{80}
Spodumene	166	276
Quartz	142	265
K-feldspars	98	223
Albite	109	242
Muscovite/lepidolite	36	144
Biotite/chlorite	8	20
Amphiboles/garnet/tourmaline	74	178
Calcite	31	106
Columbite	127	230
Sulfides	70	351
Other	28	164
Particle	132	267

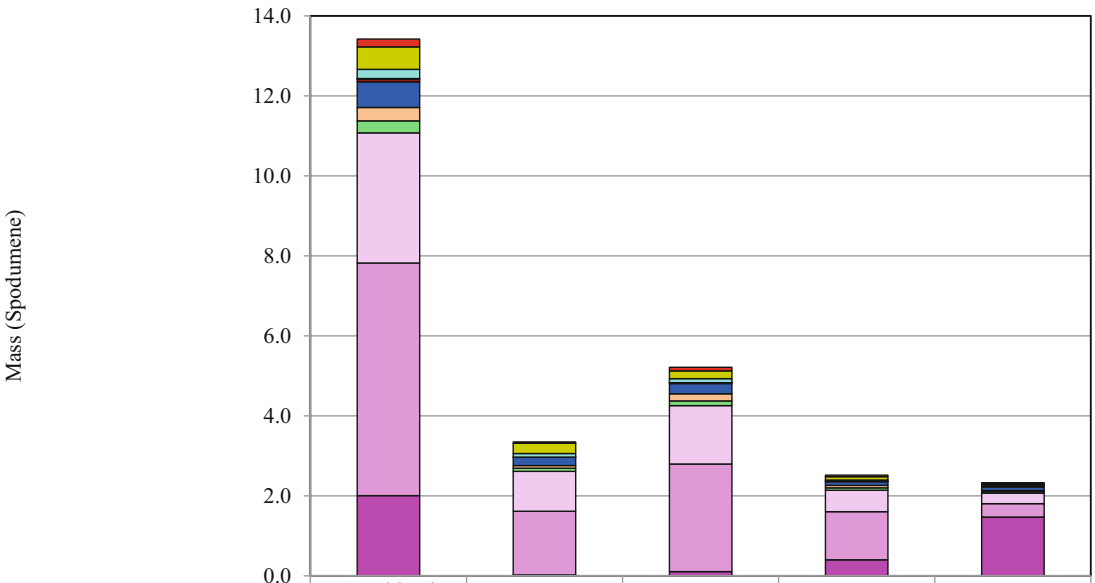

	Combined	+300 μm	-300/+150 μm	-150/+75 μm	-75 μm
Complex	0.20	0.04	0.09	0.04	0.03
Spd:Quartz/K-feldspars/Albite	0.56	0.26	0.20	0.08	0.03
Spd:Quartz/K-feldspars	0.23	0.09	0.10	0.03	0.00
Spd:Other	0.01	0.00	0.00	0.00	0.01
Spd:Biotite/Chlorite	0.01	0.00	0.00	0.00	0.01
Spd:Muscovite/Lepidolite	0.06	0.00	0.02	0.01	0.03
Spd:Albite	0.64	0.20	0.26	0.09	0.09
Spd:K-feldspars	0.33	0.07	0.17	0.06	0.03
Spd:Quartz	0.30	0.08	0.12	0.06	0.04
Lib Spodumene	3.25	1.00	1.46	0.54	0.26
Free Spodumene	5.82	1.59	2.69	1.20	0.34
Pure Spodumene	2.00	0.03	0.11	0.40	1.47

Fig. 1 Liberation and association (mass) of spodumene by size fraction and calculated head

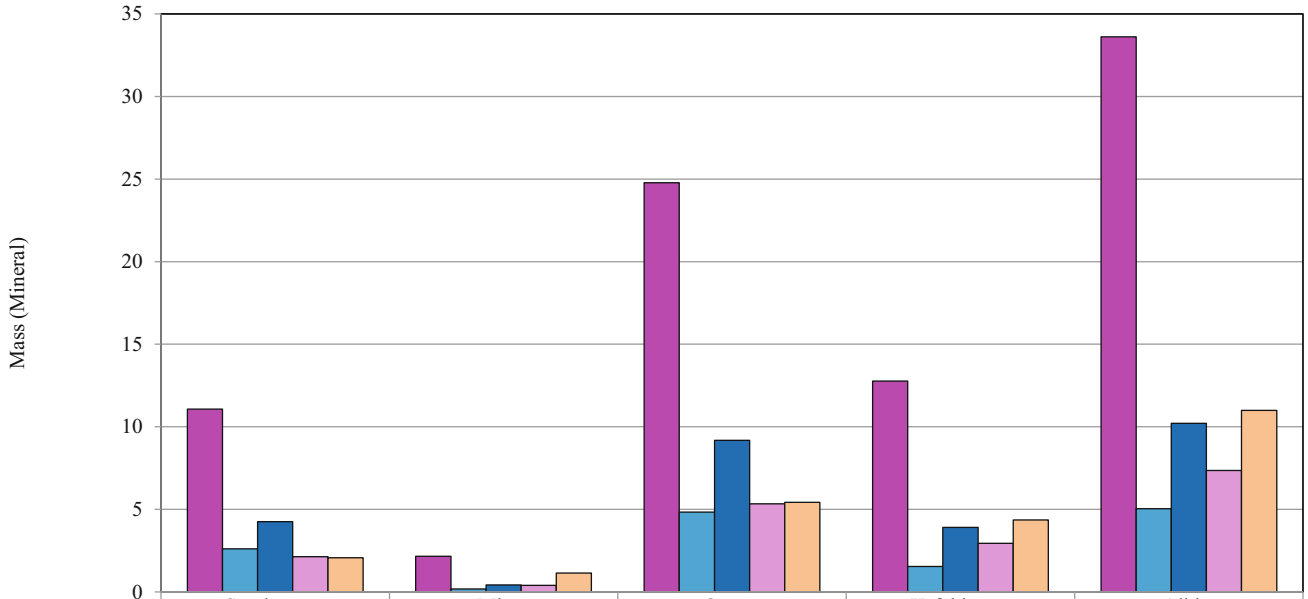

	Spodumene	Micas	Quartz	K-feldspars	Albite
Combined	11.1	2.2	24.8	12.8	33.6
+300 µm	2.6	0.2	4.8	1.5	5.0
-300/+150 µm	4.3	0.4	9.2	3.9	10.2
-150/+75 µm	2.1	0.4	5.3	3.0	7.4
-75 µm	2.1	1.1	5.4	4.4	11.0

Fig. 2 Liberation (mass) of liberated spodumene, micas, quartz, K-feldspars, and albite by size fraction and calculated head

(0.6%), quartz (0.3%), K-feldspars (0.3%), quartz/K-feldspars/albite middling (ca. 0.6%) quartz/K-feldspars (0.2%), and as complex (ternary and quaternary middling particles) (0.2%). Liberated spodumene mass accounts for 2.6% (78% by normalized mass) in the +300 µm, 4.3% in the −300/+150 µm, 2.1% in the −150/+75 µm, 2.1% in the −75 µm size fraction (or 78%, 82%, 85%, and 89% by normalized mass).

Figure 2 illustrates the liberation of spodumene, micas, quartz, K-feldspars, and albite by size fraction and calculated head. Liberated quartz accounts for 24.8% (out of 26.8%), micas (2.2% out of 3.5%), K-feldspars is 12.8% (of 15.3%), and albite is 33.6% (of 38.1%).

The lithium concentration in the spodumene was determined with LA-ICP-MS analyses. Figure 3 illustrates the theoretical grade-recovery curves for lithium as a function of the liberation of the spodumene. A lithium grade between 3.5% and 3.2% for recoveries of 70–97%, respectively, is projected for the calculated head. Note that the last two points of the curves are ignored, assuming that the spodumene with the liberation of less than 30% liberation might not be recovered. Calculations are based on the liberation and mass of the spodumene for which the highest grades and recoveries for Li are projected for −75 µm fraction while the lowest occur for the +300 µm fraction.

2.2 Mineral Chemistry and Lithium Deportment

EPMA and LA-ICP-MS show that spodumene contains an average of 3.53% lithium and 1.19% FeO. Muscovite contains an average of 3.62% FeO, 1.41% Rb_2O, 0.10% Cs_2O, and 0.29% lithium, and biotite contains an average of 0.29% Rb_2O, and 0.03% Cs_2O, and 0.43% lithium. Figure 4 illustrates the distribution of lithium-bearing minerals in the sample. The elemental deportment for lithium is calculated based on the mass of the lithium-bearing minerals, determined by TIMA-X, and their average lithium concentration, determined by LA-ICP-MS. Spodumene accounts for 0.473% of the total lithium (0.474%) in the sample. The lithium distribution indicates that (i) spodumene is the main lithium-bearing mineral; (ii) the loss of spodumene (e.g., to the tailings) is likely to be responsible for potential lithium losses in metallurgical samples.

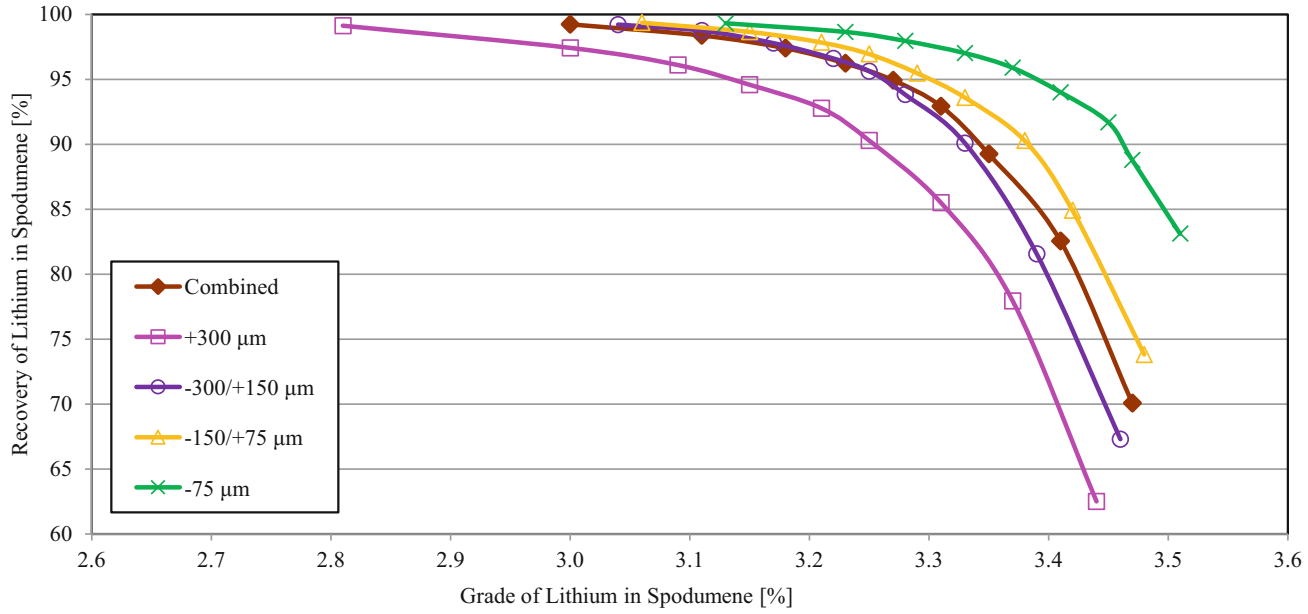

Fig. 3 Theoretical grade–recovery curves for lithium in spodumene by size fraction and calculated for the head

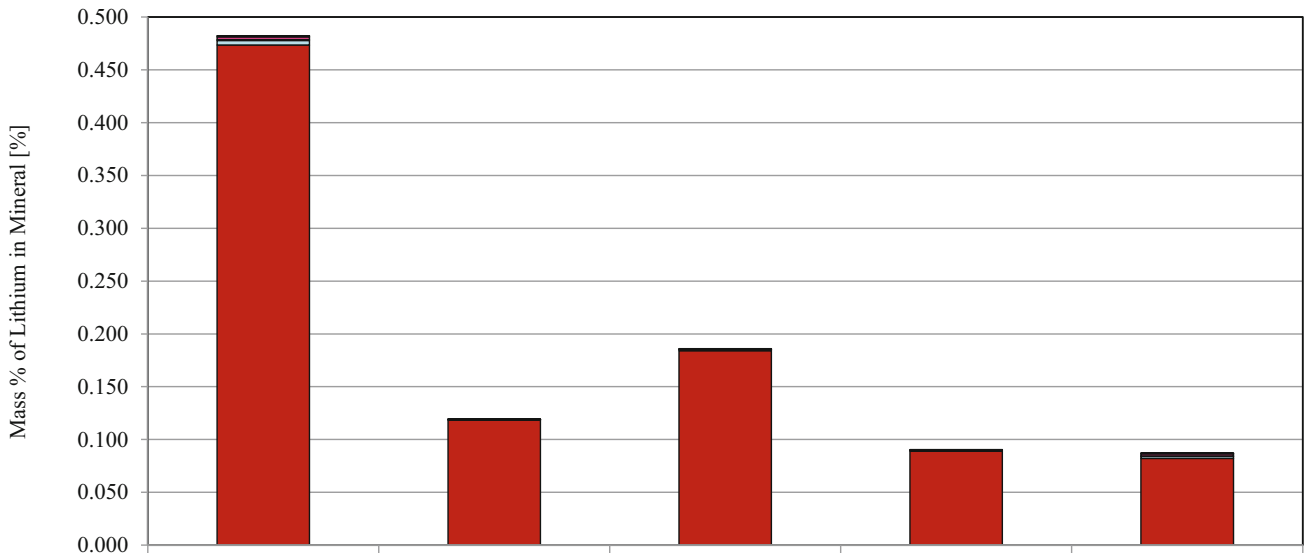

	Combined	+300 µm	-300/+150 µm	-150/+75 µm	-75 µm
Other	0.0001	0.0000	0.0000	0.0000	0.0000
Chlorite	0.0008	0.0000	0.0001	0.0001	0.0005
Biotite	0.0026	0.0001	0.0002	0.0002	0.0020
Lepidolite	0.0009	0.0001	0.0002	0.0002	0.0004
Muscovite	0.0044	0.0007	0.0011	0.0008	0.0019
Spodumene	0.4735	0.1183	0.1841	0.0889	0.0822

Fig. 4 Lithium deportment (mass) by size fraction and calculated head

3 Experimental Testwork

The ore (HG-B) was stage crushed to -6 mesh, blended, and split into 1-kg charges at SGS in Lakefield, Ontario. Eight subsamples were sent for head assays.

A 1-kg ore charge was wet screened at 180 μm or 300 μm prior to grinding followed by stage grinding at 60% solids in a laboratory rod mill to the desired product size. The two size targets used in this testwork were 100% passing 180 μm (80% passing 135 μm) and 100% passing 300 μm (80% passing 205 μm). A stainless-steel rod charge (18.4 kilograms) was used for grinding. The grind targets were based on the liberation of spodumene from the TIMA-X mineralogical analysis which yielded 78% liberation for 300 μm and 82% for −300/+150 μm.

A similar flotation schedule to what was developed by Aghamirian [16] was used in this experimental program. The samples obtained from the flotation flowsheet were assayed for lithium, silicon, aluminum, potassium, sodium, calcium, magnesium, manganese, phosphorus, and iron. The procedure consisted of high-density scrubbing and desliming. The desliming was done in a 15-liter cylinder. The settled material was used for magnetic separation and the suspension was siphoned, filtered, dried, weighed, and sent for assaying. The sediments were subjected to wet high-intensity magnetic separation (Eriez, Model # L-4-20 LAB) at a magnetic flux intensity of 9000 Gauss (5 A). The non-magnetics from the first pass were subjected to magnetic separation at a higher magnetic flux intensity of 16,000 Gauss (10 A). The magnetic concentrates were filtered, dried, weighed, and sent for analysis. The non-magnetic material from the magnetic separation was used for flotation. Flotation was done in a 4-liter cell and conditioned with sodium hydroxide to increase the pH to approximately 11 (137.5 g/t was added) followed by two mica flotation stages. The Armac T (collector) dosage used in the first and second stage of mica flotation was 80 g/t and 30 g/t, respectively. The mica concentrates were filtered, dried, weighed, and sent for analysis. The tailings from mica flotation were scrubbed at high intensity in the same flotation cell in the presence of 250 g/t F100 (dispersant from Pionera), sodium hydroxide (125 g/t) and sodium carbonate (400 g/t) followed by desliming. The desliming was done in a 15-liter cylinder. The settled material was used for flotation and the suspension was siphoned, filtered, dried, weighed, and sent for assaying. The sediments from desliming were conditioned at high density in the presence of 800 g/t FA-2 (spodumene collector from Arizona Chemical) followed by two rougher stages of spodumene flotation where the pH was adjusted to ~10 by adding 75 g/t of sodium hydroxide. After the rougher stage, the pulp was conditioned at high intensity in the presence of 150 g/t FA-2 and 25 g/t sodium carbonate (~pH 10). Lithium scavenging was then performed.

Lithium was assayed using microwave digestion, ICP-AES, and the remainder was assayed using XRF. The head assay analysis is shown in Table 3. The flotation test products and samples were split into two separate digestion streams, each independently analyzed for elemental content by ICP-AES. For silicon determination, samples were subject to a loss on ignition at 1000 C followed by lithium metaborate fusion using an electric fluxer (The Ox, Claisse). For determination of aluminum, calcium, iron, potassium, magnesium, and sodium, samples underwent microwave-induced closed vessel digestion using a multi-acid addition process, including HF. During all digestion processes and instrument calibration, duplicates and certified reference materials were used to ascertain the quality of the data reported.

4 Results

Table 3 illustrates the external reference distribution for the feed (HG-B ore). The lithium (Li) head grade was 0.47%. Most of the relative standard deviations (RSD) were less than 5% indicating that the ore was well blended.

Tables 4 and 5 show the results for the flowsheet up to the lithium rougher-scavenger flotation stage for 100% passing 180 μm and 100% passing 300 μm, respectively. For 100% passing 180 μm, the lower control limit (LCL) and upper control limit (UCL) (95% confidence) for lithium recoveries were 68.41% and 80.53% (based on feed to the flowsheet or all stages), respectively. For 100% passing at 300 μm the lower control limit and upper control limit, 95% confidence, for lithium recoveries were 68.27% and 82.20% (based on feed to the flowsheet or all stages), respectively. The 95% confidence intervals

Table 3 External reference distribution for HG-B ore

	Li (%)	SiO_2 (%)	Al_2O_3 (%)	Fe_2O_3 (%)	MgO (%)	CaO (%)	Na_2O (%)	K_2O (%)	TiO_2 (%)	P_2O_5 (%)	MnO (%)
Mean	0.474	72.09	15.39	0.759	0.279	0.759	4.33	2.94	0.050	0.024	0.090
Standard deviation	0.011	0.19	0.09	0.018	0.014	0.023	0.03	0.03	0.005	0.005	0.005
RSD (%)	2.35	0.26	0.60	2.32	4.89	3.05	0.66	1.07	10.00	20.38	5.56

Table 4 Metallurgical results (rougher flotation only) for 100% passing 180 μm

Stream	Mean Li Recovery (%)	Mean Li Grade (%)	Standard Deviation Li Recovery (%)	Standard Deviation Li Grade (%)	LCL Li Recovery (%)	UCL Li Recovery (%)	LCL Li Grade (%)	UCL Li Grade (%)
Li Ro Conc & Scav	74.47	2.11	2.44	0.17	68.41	80.53	1.69	2.54
Mica Ro & Scav	4.82	0.18	1.16	0.01	1.94	7.69	0.16	0.20
Li Ro Tails	1.10	0.01	0.23	0.00	0.53	1.68	0.00	0.02
10 A Mag Conc	4.83	1.49	1.08	0.01	2.15	7.50	1.48	1.51
5 A Mag Conc	5.60	1.14	0.81	0.03	3.58	7.62	1.07	1.21
Deslime Steps 1 & 2	9.18	0.41	0.53	0.03	7.85	10.51	0.32	0.49

Table 5 Metallurgical results for 100% passing 300 μm

Stream	Mean Li Recovery (%)	Mean Li Grade (%)	Standard Deviation Li Recovery (%)	Standard Deviation Li Grade (%)	LCL Li Recovery (%)	UCL Li Recovery (%)	LCL Li Grade (%)	UCL Li Grade (%)
Li Ro Conc & Scav	75.24	2.25	2.80	0.14	68.27	82.20	1.90	2.60
Mica Ro & Scav	5.93	0.20	0.36	0.01	5.03	6.84	0.17	0.22
Li Ro Tails	2.45	0.02	1.30	0.01	0.00	5.69	0.00	0.05
10 A Mag Conc	4.93	1.21	0.79	0.16	2.97	6.89	0.80	1.62
5 A Mag Conc	5.09	1.03	1.15	0.10	2.24	7.95	0.79	1.28
Deslime Steps 1 & 2	6.35	0.39	0.16	0.02	5.96	6.74	0.34	0.43

for the lithium grade in the rougher-scavenger concentrate for 100% passing 180 μm and 100% passing 300 μm were 1.69–2.54% and 1.90 and 2.60%, respectively. The lithium losses (95% confidence) in the mica rougher-scavenger concentrate varied from 1.94% to 7.69% for 100% passing 180 μm and 5.03–6.84% for 100% passing 300 μm. There is an overlap between the lower confidence and upper confidence limits for the grind sizes; thus, there is no significant difference in the lithium losses for the mica rougher-scavenger stage. For the magnetic field intensity of 9000 Gausses (5 A), the lithium losses varied between 3.58% and 7.62% (95% confidence) for 100% passing 180 μm and 2.24–7.95% (95% confidence) for 100% passing 300 μm. For the magnetic field intensity at 10 A (16,000 Gauss), the lithium losses varied between 2.15% and 7.50% (95% confidence) for 100% passing 180 μm and 2.97–6.89% (95% confidence) for 100% passing 300 μm. For both magnetic field intensities, the lower and upper limits overlapped, so there were no significant losses between the two grind sizes. At 100% passing 180 μm, the lower and upper confidence limits (95% confidence) for lithium recovery to the slimes, steps 1 and 2, were 7.85% and 10.51%, respectively. For 100% passing 300 μm, the lower and upper confidence limits for the deslime steps 1 and 2, 95% confidence, were 5.96% and 6.74%, respectively. The confidence limits for the lithium recovery (losses) in desliming step between the two grinds did not overlap. This implied that there was a significant difference. The *t*-test results will be discussed shortly.

The mineralogical data indicate that grades and recoveries could be improved with flotation. TIMA-X analysis is currently underway to determine the mineralogical attributes of the various flotation and magnetic products. The analysis will focus on the liberation attributes and grain size of contaminants in the concentrates, and reasons for possible losses of spodumene. Furthermore, time-of-flight (ToF) secondary ion mass spectroscopy (SIMS) is also underway to determine the surface chemistry characteristics of the various minerals. This investigation will focus on the reasons for the response of the minerals due to collectors and reagents. A combination of the TIMA-X and ToF-SIMS will explain the response of the minerals in the various metallurgical products.

Table 6 *t*-test for lithium recoveries

Li Recovery (%) for 100% passing 180 μm	Li Recovery (%) for 100% passing 300 μm
77.17	72.06
73.84	77.38
72.42	76.26
Mean = 74.47	Mean = 75.23
Standard deviation = 2.44	Standard deviation = 2.80

Table 7 *t*-test for lithium recoveries in deslime steps

Li Recovery (%) for 100% passing 180 μm	Li Recovery (%) for 100% passing 300 μm
8.79	6.18
9.79	6.41
8.97	6.48
Mean = 9.18	Mean = 6.35
Standard deviation = 0.53	Standard deviation = 0.16

Table 6 illustrates the analysis of a 2-sample *t*-test between 100% passing 180 μm and 100% passing 300 μm in terms of their respective lithium recoveries during the lithium rougher-scavengers. The difference in the average lithium recoveries between the two grind sizes was small; thus, a two-sample *t*-test was done for the lithium recoveries to determine whether this difference was significant. The critical *t*-value at 95% confidence with four degrees of freedom was 2.776 (from the *t*-distribution table-[17]). The calculated *t*-value from data in Table 6 was −0.134. The method to calculate these parameters can be found in [17]. Since the calculated *t*-value does not exceed the critical *t*-value, the lithium recoveries between the grind sizes were not significantly different or there are not enough available evidence to reject the null hypothesis that there is no difference in the lithium recovery between the two grind sizes. Table 7 illustrates the analysis of a 2-sample *t*-test for 100% passing 180 μm and 100% passing 300 μm for lithium recoveries in the desliming steps. The calculated *t*-value (8.81) exceeds 2.776; thus, the difference between the lithium recoveries in the deslime steps between the two grinds was significant. At 100% passing 180 μm, more lithium was lost in the desliming steps.

5 Discussion

The lithium recoveries difference between the two grind sizes was not significant; this finding agreed with spodumene liberation and projected recoveries of lithium and spodumene as discussed in the mineralogical section. However, more lithium was lost in the slimes (desliming steps) for the 100% passing 180 μm grind. This can be attributed to the higher settling time of the slime at this grind size resulting in higher losses. The mineralogical analysis was done on various size fractions (+300, −300/+150, −150/+75, and −75 μm). For the −300/150 μm and −150/+75 μm size fractions, the spodumene liberations were 81.6% and 84.9%, respectively; the liberation for these size fractions was similar. Thus, grinding the ore at 100% passing 300 μm and 100% passing 180 μm would result in a similar degree of liberation of lithium resulting in insignificant lithium recovery differences between the two grind sizes.

Grinding the ore to 100% passing 300 μm rather than 100% passing 180 μm will result in much lower energy costs and lower capital costs for Sayona Lithium. Furthermore, lower energy consumption will result in lower green gas emissions.

6 Conclusions

For the lithium ore sample studied in this case study, its primary lithium mineral is spodumene, accounting for 0.47% (or 98%) of the total lithium in the sample. The absence of phosphates and the low mica grades which may carry variable amounts of lithium are beneficial for the project.

Liberated spodumene accounts for 11.1% (out of the 13.4% of the total mass or ca. 83% by normalized mass in the sample, and increases by 11% from 78% in the coarse (+300 μm) to 89% in the fine (−75 μm) size fraction.

Based on the mineralogical analysis, the liberation between the sizes tested (100% passing 180 μm and 100% passing 300 μm) was similar.

Mineralogical analysis yields lithium grades, calculated for the head sample, between 3.5% and 3.2% for recoveries of 70–97%, respectively. Lithium grades and recoveries between the +300 µm and −300/+150 µm size fractions are similar based on the mineralogical analysis given the small difference in the liberation of spodumene between these two fractions.

The lithium recoveries in the lithium rougher-scavenger flotation concentrate between the sizes tested (100% passing 180 µm and 100% passing 300 µm) were not significantly different or not enough evidence to reject the null hypothesis (no difference in lithium recoveries between the grind sizes).

The lithium recoveries in the desliming steps between the sizes tested (100% passing 180 µm and 100% passing 300 µm) were significantly different.

Additional mineralogical and mineral surface analyses are underway to better understand the response of the minerals in the various metallurgical products.

Acknowledgments This work was funded by CanmetMINING, Natural Resources Canada, under the Critical Minerals Research, Development and Demonstration Program. The authors would like to thank, Soha Issa, Jaime Ferreira, Samir Samhat, and Brandon Wang at CanmetMINING for their work in the laboratory and the analytical laboratory at CanmetMINING. We also thank SGS Canada for the logistical support.

References

1. National Academy of Sciences (2021) Global warming is contributing to extreme weather events | National Academies, https://www.nationalacademies.org
2. Tadesse B, Makuei F, Albijanic B, Dyer L (2019) The beneficiation of lithium minerals from hard rock ores: a review. Miner Eng 131:170–184
3. Sousa R, Ramos V, Guedes A, Botelho de Sousa A, Noronha F, Machado Leite M (2019) Flotation of lithium ores to obtain high-grade Li_2O concentrates. Are there any mineralogical limitations? Int J Mini Mater Metallur Eng 5:7–18
4. Penner SS (1977) Lithium needs and resources. Corning, New York
5. Goodenough JB, Park KS (2013) The Li-ion rechargeable battery: a perspective. J Am Chem Soc 135:1167–1176
6. Dunn B, Kamath H, Tarascon JM (2011) Electrical energy storage for the grid: a battery of choices. Science 334:928–935
7. Reichel S, Aubel T, Patzig A, Janneck E, Martin M (2017) Lithium recovery from lithium-containing micas using sulfur oxidizing microorganisms. Miner Eng 106:18–21
8. Chagnes A, Swiatowska J (2015) Lithium process chemistry: resources, extraction, batteries, and recycling https://doi.org/10.1016/C2013-0-19081-2
9. Bulatovic SM (2014) Beneficiation of lithium ores. In: Bulatovic SM (ed) Handbook of flotation reagents: chemistry, theory and practice – volume 3: flotation of industrial minerals. Elsevier B.V, pp 41–56
10. Fuerstenau MC, Miller JD, Kuhn MC (1985) Flotation fundamentals. Marcel Dekker Inc, New York/Basel
11. Amarante MM, Botelho de Souza A, Machado Leite M (1999) Processing a spodumene ore to obtain lithium concentrates for addition to glass and ceramic bodies. Miner Eng 12:433–436
12. Menéndez M, Vidal A, Toraño J, Gent M (2004) Optimisation of spodumene flotation. Eur J Miner Process Environ Prot 4:130–135
13. Grammatikopoulos T, Aghamirian M, Fedikow M, Mayo T (2020) Mineralogical characterization and preliminary beneficiation of the Zoro Lithium Project, Manitoba, Canada. Mining Metallurgy Explor 38:329–346
14. Grammatikopoulos TA, Pearse G, Gelcich S, Gunning C (2009) Quantitative characterization of spodumene ore by automated mineralogy from the Moblan rare Metals pegmatite Deposit, Quebec, Canada. Proceedings of the 48th annual conference of metallurgists of CIM (MetSoc), pp 65–76
15. Aylmore MG, Merigot K, Rickard WDA, Evans NJ, McDonald BJ, Catovic E, Spitalny P (2018) Assessment of a spodumene ore by advanced analytical and mass spectrometry techniques to determine its amenability to processing for the extraction of lithium. Miner Eng 119:137–148
16. Aghamirian M, Saad AS, McCarley R (2018) An investigation into flotation pilot plant testing Authier Lithium Project, August 7th. SGS, Lakefield, Ontario
17. Kiemele MJ, Schmidt SR, Berdine RJ (1997) Basic statistics, tools for continuous improvement, 4th edn. Air Academy Press